

## Proceedings of the Eurosensors XXIII conference

## Nanogaps for Sensing

Frédéric Favier<sup>a</sup>*a Institut Charles Gerhardt, AIME, UMR 5253 CNRS, Université Montpellier II, cc015 34095 Montpellier Cedex 5, France*

---

**Abstract**

Modern resistive chemical sensors include discontinuous nano/mesostructures. Sensing performances are then governed by the chemical nature of the nanostructure gap as well as by the sensor design at the nanogap scale. Various top-down, bottom-up and hybrid fabrication routes of discontinuous/nanogaped metal nano and mesostructures have been developed. These structures are assembled/organized on insulating surfaces for integration of resistor based devices for the specific sensing of chemicals in gaseous as well as in liquid media. Hydrogen sensing based on discontinuous/gaped palladium nano/mesostructures is a chosen case-study for the evaluation of various nano/mesogap fabrication methods.

Keywords: nano/mesogap fabrication; top-down; bottom-up; hybrid method; chemical sensing

---

**1. Introduction**

In several sensing devices, sensitive part includes separated elements or gaps. Depending on the device type, span size can range from micrometers to nanometers and progressively tend to decrease for miniaturisation purpose, performance improvement or simply because of a sensing mechanism based on the presence of discontinuities or gaps. Gap micro or nanostructures can be found in microelectromechanical systems (MEMS) such as accelerometer or pressure gauges.<sup>1</sup> An Atomic Force Microscopy (AFM) tip running in non-contact mode is a cutting-edge example of such gap-based mechanical sensors. In contrast, air-bag actuators in modern cars are probably the most widely spread MEMS based on separated elements. On the other hand, chemio-resistive sensing devices are based on the variation of the electrical conductivity of the sensing material when interacting with the targeted analyte.<sup>2</sup> Sensing operation imposes the use of electrodes with span tending to nanosize as single molecule based devices are now being envisioned. For some other resistive chemical sensors, the sensitive part itself has to include gaps and discontinuities. This is typically the case for hydrogen sensors based on discontinuous palladium nano/mesostructures. Sensing mechanism is based on reversible gap closing/opening under H<sub>2</sub>/H<sub>2</sub>-free atmospheres undergoing the conversion equilibrium between palladium and corresponding palladium hydride.<sup>3,4</sup> Sensing performances depend on device designs and material microstructures and assembling/organizations. Various top-down, bottom-up and hybrid fabrication routes of discontinuous palladium structures can be used for the fabrication of such resistor based H<sub>2</sub> sensing devices. 1-D, 2D, and 3-D structures can be achieved using appropriate material templating and self-organization methods constituting an appropriate case study for the evaluation of potential fabrication methods of nanogaps for sensing.

---

<sup>a</sup> Corresponding author. Tel.: +33-467143332; fax: +33-467143304.

E-mail address: [fredf@univ-montp2.fr](mailto:fredf@univ-montp2.fr).

## 2. Results and Discussion

### 2.1. Top-down route: A single nanotrench in an evaporated palladium microwire

The selected top-down engineering approach explores advantages and limits of the use of reliable, repeatable and scalable lithography -based fabrication method for the perfect control of the number and the geometrical arrangement of nanogaps between two electrodes. A large set of material deposition techniques is available while the choice of the most suitable substrate is expected to simultaneously improve sensing performances and facilitate system integration procedures.<sup>5</sup>

Palladium microwires of various thicknesses were fabricated by e-beam evaporation at room temperature and lift-off process (figure 1-left) onto various insulating layers including SiO<sub>2</sub> (rigid) and polyimide (PI, elastic). A single nanotrench was fabricated by focused ion beam milling (FIB) in evaporated palladium microwires. As shown in Fig.1, trenches of different nominal widths were milled into wires. Single FIB cuts were performed using milling doses in the range of 1–2 (nm<sup>2</sup>s)<sup>-1</sup> and 1.7–2.7 (nm<sup>2</sup>s)<sup>-1</sup> to completely open gaps in air.

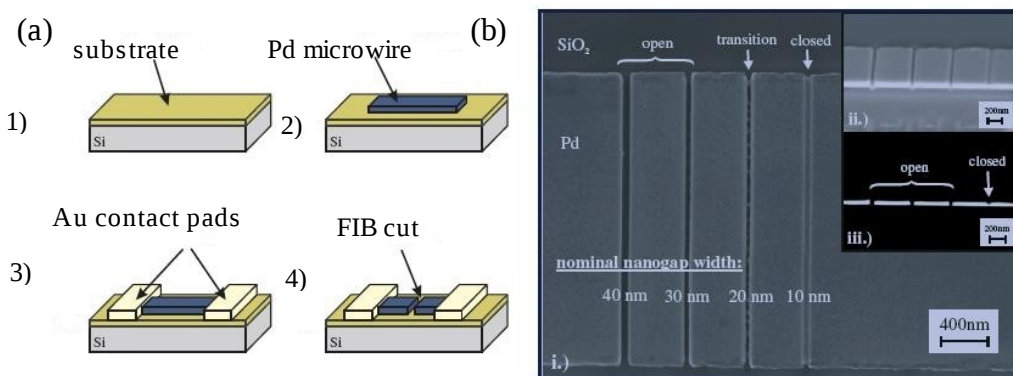


Fig. 1. (a) Schematic process flow for fabrication of the sensing devices; (b) Analysis of four exemplary nanotrenches by SEM. (i) FIB cuts with different nominal widths (from left to right: 40, 30, 20, 10 nm) in a 50 nm thin Pd microwire, (ii) FIB milled cross section of the same trenches, (iii) the same image but with enhanced contrast. The images show open cuts, a partially open cut and a cut on the onset of milling.

Microwires on SiO<sub>2</sub> peeled off after a few H<sub>2</sub>/N<sub>2</sub> cycles. These damages are caused by the high mechanical stress, on the order of several Gpa, induced by the Pd to PdH<sub>x</sub> conversion in the thin microwire.<sup>6</sup> As shown in Fig.2, on PI substrate both 25 and 50 nm thick wires showed closing effects under H<sub>2</sub>/N<sub>2</sub> atmospheres.

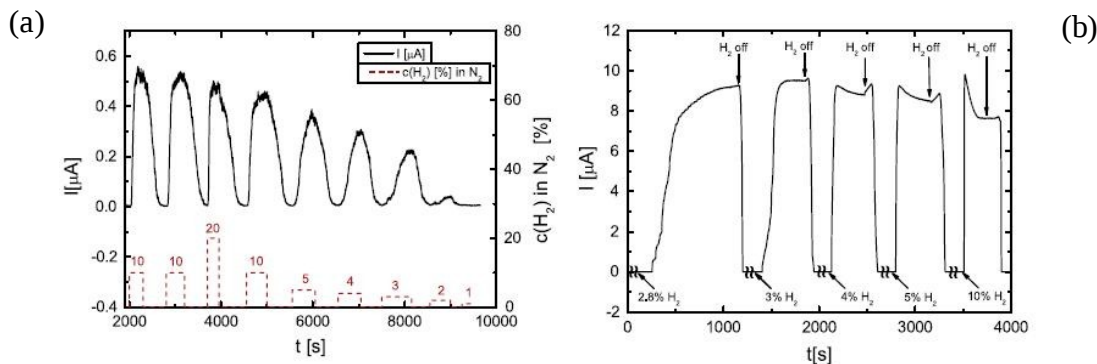


Fig. 2. (a) Typical electrical signal a FIB-cut Pd microwires on PI coating and a single nanotrench under various H<sub>2</sub>/N<sub>2</sub> cycles (room temperature, bias = 20 mV); (b) 25 nm thick Pd wire, trench width: 61 nm ± 5 nm; (b) 50 nm thick Pd wire, trench width: 26 nm ± 5 nm. The superposition of the mechanical closing of the gap (resulting in an increase in current) and the change in resistance due to the conversion of Pd to PdH<sub>x</sub> (resulting in a decrease in current) become visible at H<sub>2</sub> concentrations above 3%. No response was observed for H<sub>2</sub> concentrations below 2.5%.

## 2.2. Bottom-up approach: Electrochemical synthesis and 1D and 3D palladium particles assembles for $H_2$ detection

**Electrodeposited arrays of palladium and silver-palladium mesowires:** Arrays of palladium or silver-palladium mesowires were obtained by electrochemical decoration of step-edges present at pyrolytic polycrystalline surfaces (HOPG).<sup>3,4</sup> Arrays were then transferred onto a non-conductive substrate. Palladium and silver-palladium mesowire arrays were operated as  $H_2$  sensor by applying a constant voltage of a few mV between evaporated gold contacts and measuring the corresponding 1–20  $\mu A$  current. As shown in Fig. 3, the resistance of the sensor decreased in the presence of  $H_2$ . This decrease was related to  $H_2$  concentration, with a proportional detection in the range from 12 to 0.5%  $H_2$  in  $N_2$  for pure palladium-based sensor.

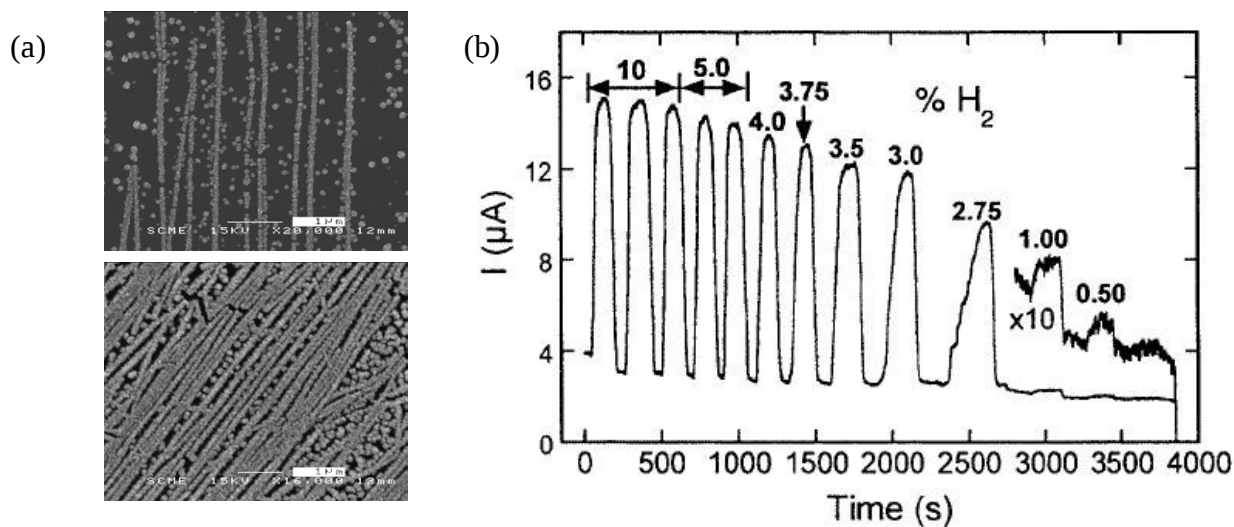


Fig. 3. (a) SEM microographies of electrodeposited Pd-Ag mesowires at 15%Ag in Pd (top) and 20%Ag in Pd (bottom); (b) Current response of a palladium mesowire-based  $H_2$  sensor under exposure to hydrogen/nitrogen mixtures (concentration of  $H_2$  as shown).

Perfectly suited for safety purpose, the limited detection range from 12 to 0.5%  $H_2$  in  $N_2$  has been extended to full concentration range from 0.5 to nearly 100% using mesowires made of PdAg alloys of various compositions (Fig.3(a)).

**Disorganised palladium particles 3D assembles for  $H_2$  detection**<sup>7</sup>: In this approach, palladium nanoparticles were electrochemically generated by reduction of an anhydrous metal salt solubilized in a polar organic medium. This preparation method developed by Reetz is perfectly suited for the preparation of stable metal colloids.<sup>8</sup> An alkylammonium surfactant simultaneously acts as electrolyte support as well as colloid stabilizer. Concentrated Pd colloids are obtained by electrochemical reduction under controlled atmosphere of a Pd salt (4mM  $PdCl_2$ ) in 0.1M tetraoctylammoniumbromide/dry THF electrolyte. Ad-atoms generated at the cathode form small clusters which are quickly stabilised by the cationic surfactant. Particle size from 2 to 10nm can be tuned by controlling the applied current density (in the range of a few  $mAcm^{-2}$ ). The larger the current density, the smaller the particles. By slow evaporation of the solvent, microsyzed aggregates were deposited onto a glass or silicon surface. Device integration was achieved using metal contacts obtained by sputtering through a designed stencil mask allowing electrical measurements.

## 2.3 Hybrid approach: Surface organization of overgrown palladium islands with nanoscale gap separations.

This hybrid route proceeds by electrochemical deposition of palladium islands on highly doped N-type silicon through a pre-patterned insulating layer.<sup>9</sup> Surface patterning is achieved through the fabrication of a lithographically engineered insulating layer onto the electrode surface. Template design consists in 2D hexagonal arrangement of holes through an insulating layer with nominal inter-hole distances and hole diameters in the range of few tens of nanometers. Pd electrodeposition has been performed for a controlled overgrowth at the insulator surface while

keeping few nanometer gap separations from islands to islands. A 2-4mM  $\text{PdCl}_2$  aqueous solution in hydrochloric electrolyte is used to perform this electrochemical step. Gold contacts are evaporated through metal masks to allow sensing measurements. Figure 6 shows a SEM image of the sensing surface as insert of the current response vs time of the corresponding sensor under  $\text{H}_2/\text{N}_2$  flows at low  $\text{H}_2$  concentrations. Detection signal is proportional in a large concentration range from 0.1% to 50% of  $\text{H}_2$  in  $\text{N}_2$  due to the gap size distribution arising from the high surface roughness of polycrystalline Pd islands obtained using these electrolysis parameters. As for sensors fabricated by other bottom-up or top-down approach, measured response and recovery times are fast and sensors can be cycled over a large number of  $\text{H}_2/\text{H}_2$ -free cycles.

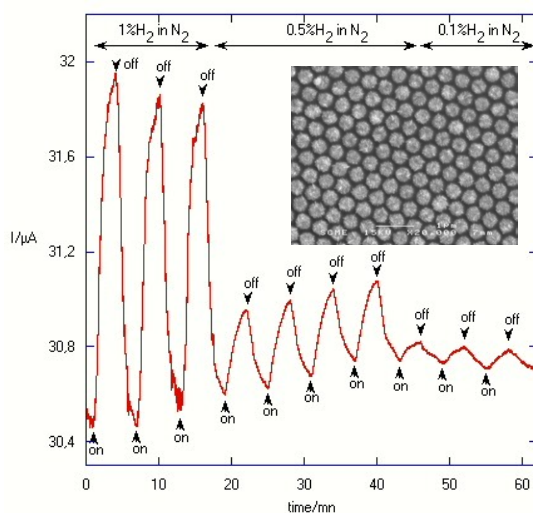


Fig. 4. Response of a Pd island based sensor fabricated by hybrid approach (20mV bias) at low concentrations of  $\text{H}_2$  in  $\text{N}_2$  and SEM micrograph of the sensitive part.

### 3. Acknowledgments

The author would like to acknowledge the technical support from the Center of MicroNanotechnology (CMI) in Lausanne and Michel Ramonda from LPCP (Laboratoire de Microscopie en Champ Proche), UM-II in Montpellier, for AFM measurements under hydrogen. Financial support from the FP6 Integrated Project HySYS SES6-019981 and from Peugeot-Citroen-Automobile (PCA) is gratefully acknowledged. Parts of this project have been developed within the frame-works of two international exchange programs co-funded by NSF and CNRS (UC Irvine (R.M. Penner) – Université Montpellier 2 collaboration) and Swiss and French governments through Germaine de Stael program (Ecole Polytechnique Fédérale de Lausanne (J. Brugger) – Université Montpellier 2 collaboration)

### 4. References

1. S.P. Beeby, N.J. Grabham, N.M. White, *Sensor Review*, **21**, 1, 33-7, 2001
2. M.E. Franke, T.J. Koplin, U. Simon, *Small* **2006**, **2**, 1, 36-50
3. F. Favier, E. Walter, T. Benter, and R.M. Penner. *Science*, Sept 21, 2227, 2001.
4. E. Walter, F. Favier, and R.M. Penner. *Analytical chemistry*, **74**, 1546, 2002.
5. U. Laudahn, S. Faehler, H.U. Krebs, A. Pundt, M. Bicker, U.V. Huelsen, U. Geyer, and R. Kirchheim, *Appl. Phys. Lett.*, **74**, 647, 1999.
6. T. Kiefer, F. Favier, O. Vazquez-Mena, G. Villanueva, and J. Brugger, *Nanotechnology*, **19**, 125502, 2008.
7. F.J. Ibanez and F.P. Zamborini, **22**, 23, 9789, 2006.
8. M.T. Reetz and M. Maase, *Adv. Mater.*, **11**, 9, 773, 1999.
9. F. Favier, J. Brugger, and J.-F. Ranjard, French patent application #0757673, 09/19/2007.